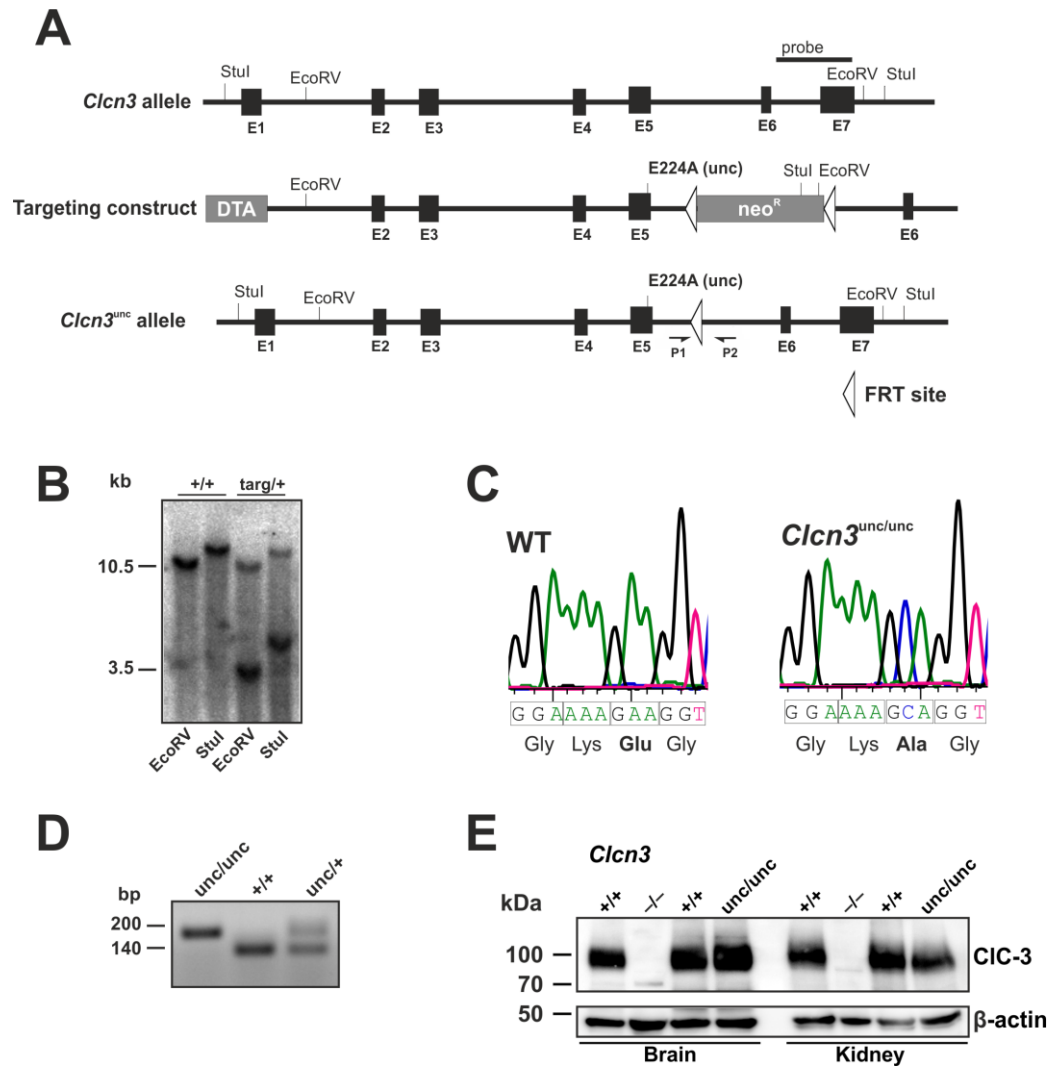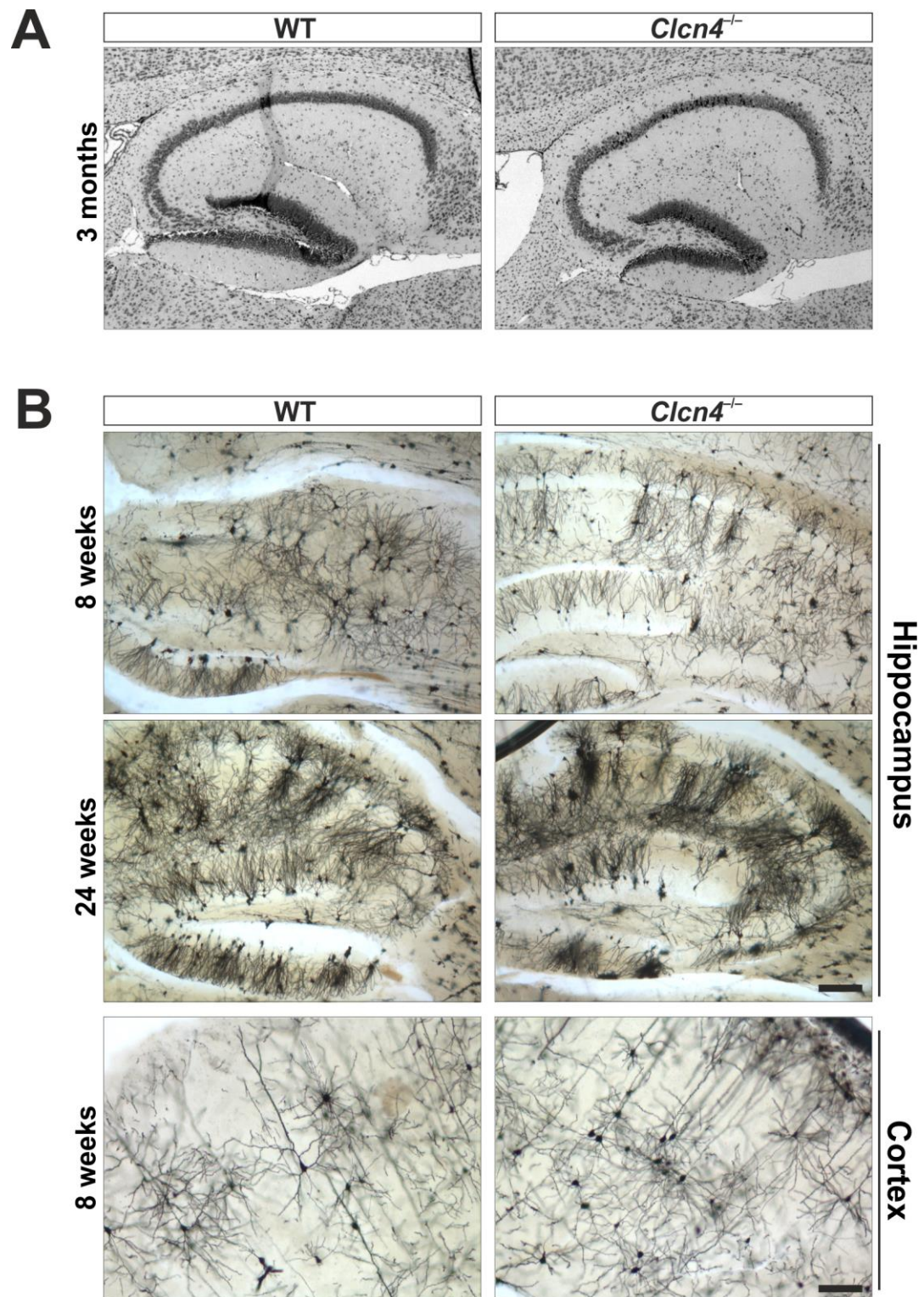# Appendix

Uncoupling endosomal proton from chloride transport causes severe neurodegeneration

Stefanie Weinert, Niclas Gimber, Dorothea Deuschel, Till Stuhlmann,

Dmytro Puchkov, Zohreh Farsi, Gaia Novarino, Carmen F. Ludwig,

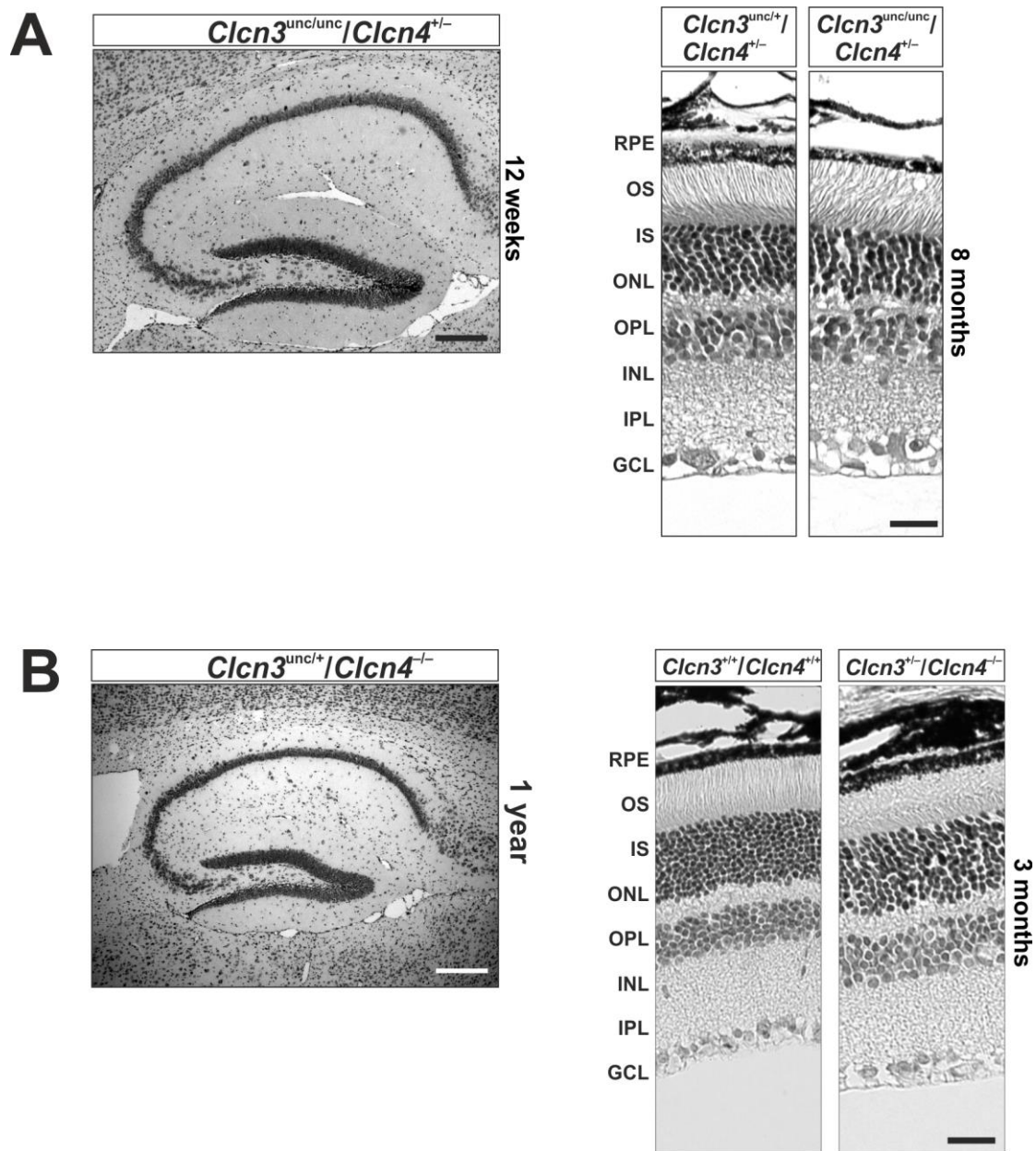Karen I. López-Cayuqueo, Rosa Planells-Cases, Thomas J. Jentsch
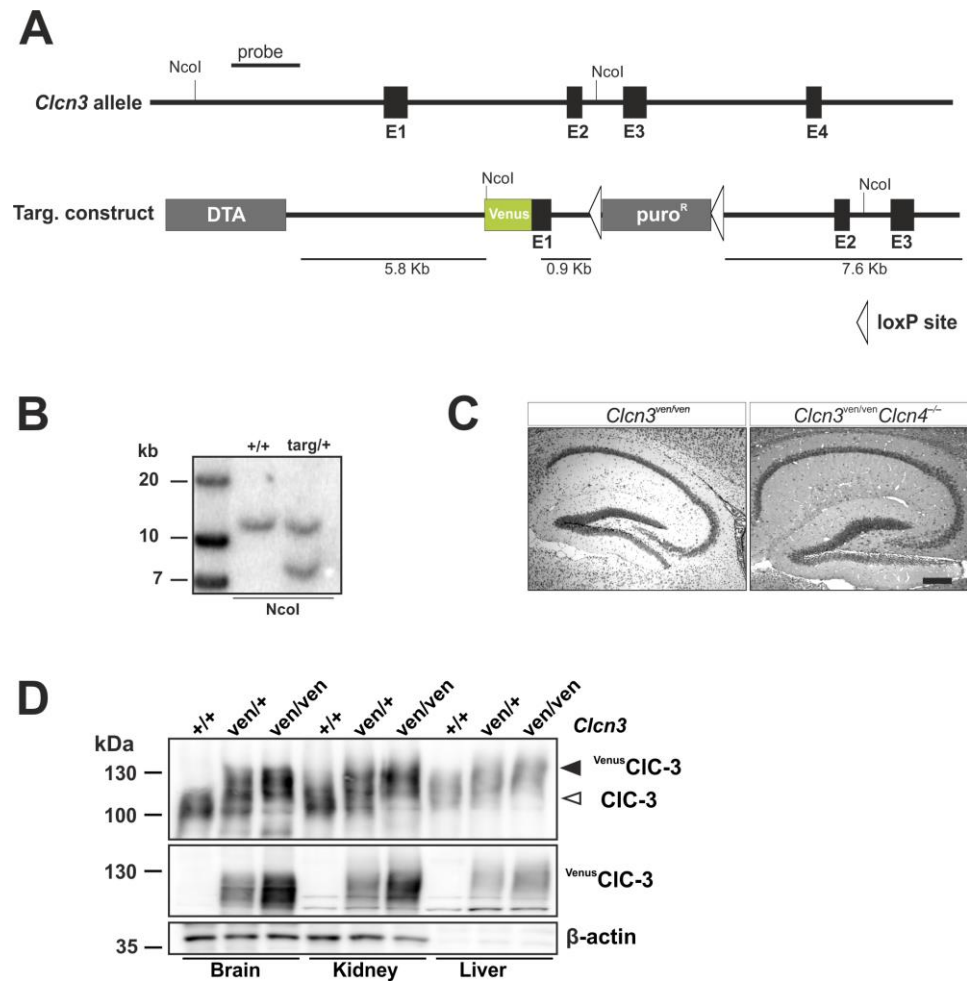
Appendix Figures S1 – S6

Appendix Figure S1. Generation of Clcn3^{unc/unc} mice. (**A**) The targeting construct contains 11.7 kb of mouse genomic sequence encompassing exons 2 through 6 with a DTA (diphtheria toxin A) cassette added to one end to select for homologous recombination. Exon 5 was modified by introducing a point mutation resulting in E224A exchange. A neomycin resistance (neo^R) cassette (flanked by FRT sites) was inserted between exon 5 and 6 as selection marker. Correctly targeted embryonic stem (ES) cells were injected into blastocysts. Chimeric animals were crossed with FLPe-recombinase-expressing 'deleter' mice[1] resulting in the Clcn3^{unc} allele (bottom). (**B**) Mouse genomic ES cell DNA was digested with EcoRV or StuI for Southern blot analysis. Positive clones were identified with an external hybridization probe shown in (A). (**C**) DNA sequence obtained from homozygous Clcn3^{unc/unc} mice confirmed the presence of the E224A mutation. (**D**) PCR on mouse genomic DNA was used for genotyping. The sequence of the PCR primers shown in (A) were for P1: 5' GCATTTTCCTAGCAGGTG 3' and for P2: 5' AAGACTCCCAGAGACAATGAG 3'. (**E**) Western blot for ClC-3 of membrane fractions isolated from brain and kidney of WT (+/+), Clcn3^{–/–} (–/–) and Clcn3^{unc/unc} (unc/unc) mice. β-actin, loading control.

Appendix Figure S2. No anatomical changes in brain sections of *Clcn4*−/− mice. (A) Nissl-stained sagittal brain sections reveals normal hippocampal morphology of 3-months-old *Clcn4*−/− mice. (**B**) No obvious changes in neuronal anatomy in hippocampus and cortex of 8- and 24–weeks-old *Clcn4*−/− mice as determined by Golgi-Cox staining (scale bar upper panel: 200 μm, scale bar lower panel: 100 μm).
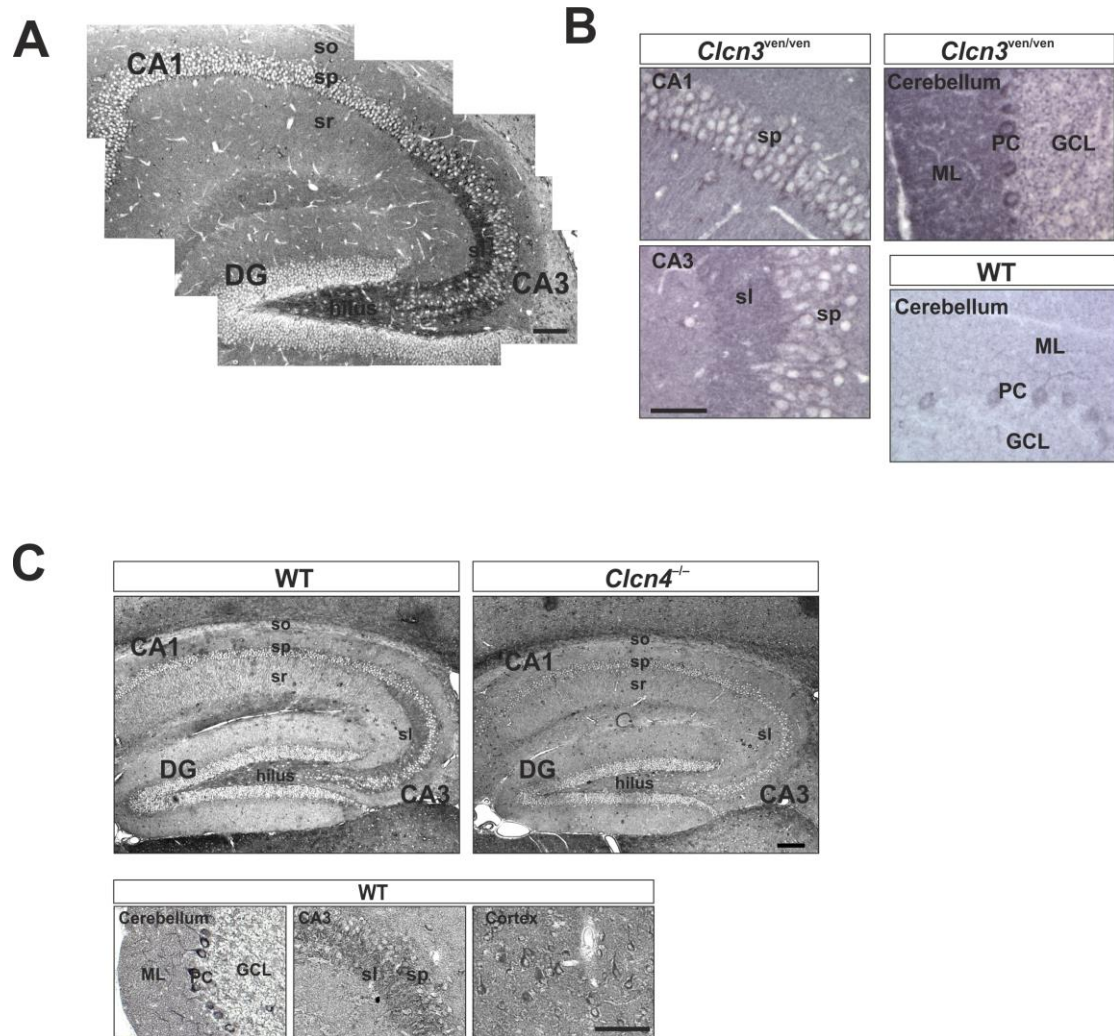
Appendix Figure S3. Brain and retina histology of heterozygous *Clcn3*/*Clcn4* mouse models. (**A**) Nissl stained paraffin sections of a 12-weeks-old brain and 8-months-old retinae showed neuronal degeneration neither in *Clcn3*^unc/unc^/*Clcn4*^+/−^ nor in *Clcn3*^unc/+^/*Clcn4*^+/−^ mice (scale bar: left: 200 μm; right: 100 μm). (**B**) Representative Nissl staining showed normal morphology of the hippocampus of a 1-year-old *Clcn3*^unc/+^/*Clcn4*^−/−^ mouse (scale bar: 200 μm). Nissl-stained paraffin sections of 3-months-old retinae showed no retinal degeneration in *Clcn3*^+/−^*Clcn4*^−/−^ mice (scale bar: 100 μm). RPE, retinal pigment epithelium; OS, photoreceptor outer segments; IS, photoreceptor inner segments; ONL, outer nuclear layer; OPL, outer plexiform layer; INL, inner nuclear layer; IPL, inner plexiform layer; GCL, ganglion cell layer.
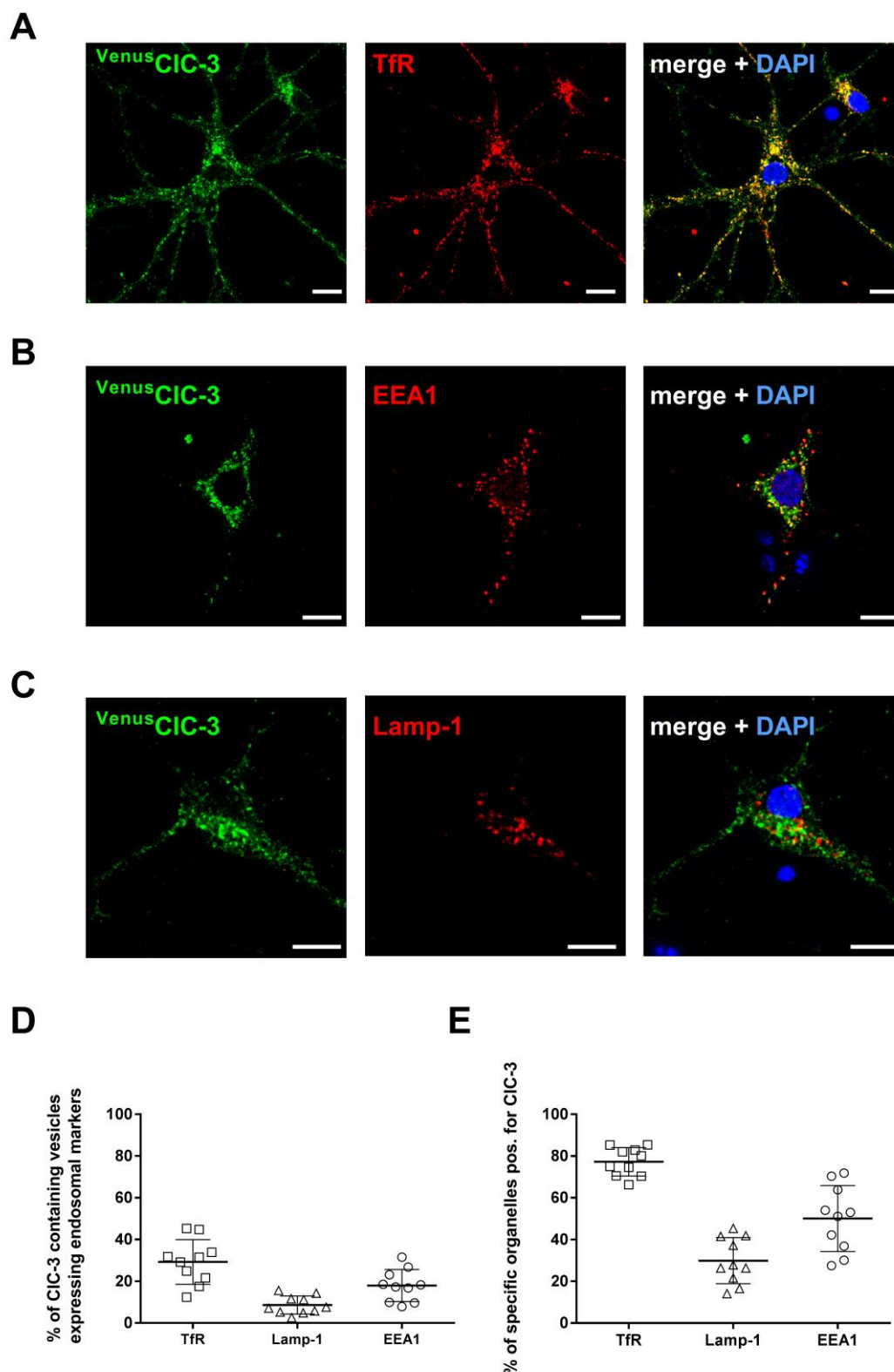
Appendix Figure S4. Generation of *Clcn3*^{ven/ven} mice. (**A**) Strategy for generation of the ClC-3^{Venus} KI mutation in mouse embryonic stem cells. The WT *Clcn3* allele and the targeting vector are shown. The targeting construct contains 14.3 kb of mouse genomic sequence encompassing exons 1 through 3 (exons are indicated by black boxes) with a DTA (diphtheria toxin A) cassette added to one end to select for homologous recombination.

A puromycin (puro^R) resistance cassette flanked by loxP sites was introduced between exon 1 and 2 to select for recombination in ES cells. Venus cDNA (indicated by a green box) was inserted by recombinant PCR onto the start ATG of the *Clcn3* ORF. A silent point mutation was introduced to generate an NcoI restriction site for subsequent Southern blot analysis. (**B**) Mouse genomic ES cell DNA was digested with NcoI for Southern blot analysis. Positive clones were identified with an external hybridization probe shown in (a). (**C**) Nissl staining show normal morphology of the hippocampus and retina of 10–weeks-old *Clcn3*^{ven/ven} and *Clcn3*^{ven/ven}/*Clcn4*^{−/−} mice (scale bar: 200 μm). (**D**) Immunoblots comparing ^{Venus}ClC-3 and ClC-3 expression in brain, liver and kidney membrane fractions isolated from WT (+/+), *Clcn3*^{ven/+} (ven/+) and *Clcn3*^{ven/ven} (ven/ven) mice. In the upper panel we used an antibody against ClC-3 for detection, whereas the middle panel we used an anti-GFP antibody which only reveals ^{Venus}ClC-3. Note that the Venus-ClC-3 protein runs at a higher molecular weight due to the fusion of the Venus tag. β-actin served as a loading control.

Appendix Figure S5. Cellular localization of ^{Venus}ClC-3 and ClC-4 in mouse brain. (A) Dark immunostaining showed ^{Venus}ClC-3 expression in the hippocampus, which is particularly strong in the CA3 region and the hilus. (**B**) Dark immunolabelling of ^{Venus}ClC-3 in cell bodies of pyramidal cells in hippocampal CA1 and CA3 region, hippocampal stratum lucidum (sl) and cell bodies of cerebellar Purkinje cells (PC) and throughout the molecular layer (ML). Scale bars: (A) 1 mm and (B) 0.5 mm). (**C**) Dark immunostaining showed strong expression of ClC-4 in the hilus and stratum lucidum of the hippocampus in *Clcn4$^{+/+}$* mice that was absent in *Clcn4$^{-/-}$* mice. Additionally strong immunostaining can be observed in the cell bodies of cerebellar Purkinje cells and pyramidal cells of the hippocampal CA1 region and in the cortex (scale bars: (upper panels) 1 mm and (lower panels) 0.5 mm). Molecular layer, ML; sp, stratum pyramidale; so, stratum oriens; sr, stratum radiatum; DG, dentate gyrus; GCL, granular cell layer; PC, Purkinje cells.

Appendix Figure S6. Cellular localization of ^{Venus}ClC-3 in cultured hippocampal neurons. (A-C) Confocal images to reveal co-localization of ^{Venus}ClC-3 with the transferrin receptor (TfR) (A), the endosomal marker protein EEA1 (B) and the late endosomal/lysosomal marker Lamp-1 (C). Cultured hippocampal neurons from

Clcn3^{venus/venus} mice were immunolabeled with antibodies against GFP (to detect the Venus protein) and the respective marker proteins. Scale bar represents 10 μm. (**D**) Percentage of ^{Venus}ClC-3-positive structures that are also positive for TfR, EEA1 or Lamp-1. (**E**) Percentage of structures positive for the indicated marker proteins that are also positive of ^{Venus}ClC-3. Images were processed and quantified in Image J. Manders' coefficients co-localization analysis were performed in regions of interests that represent neuronal somata using JACoP (Just Another Co-localization Plug-in) for Image J. Results were obtained from 10 cells from two different animals each. Data are presented as mean ± SD.